

ORIGINAL ARTICLE

Structure and Innervation of the Equine Supraspinous and Interspinous Ligaments

A. Ehrle^{1*}, L. Ressel², E. Ricci² and E. R. Singer³

Addresses of authors: ¹ Philip Leverhulme Equine Hospital, Institute of Veterinary Science University of Liverpool, Chester High Road, Neston, CH64 7TE, UK;

² Section of Veterinary Pathology, Institute of Veterinary Science University of Liverpool, Chester High Road, Neston, CH64 7TE, UK;

³ Institute of Ageing and Chronic Disease University of Liverpool, 6 West Derby Street, Liverpool, L7 8TX, UK

***Correspondence:**

Tel.: +44 (0) 151 794 6041;

Fax: +44 (0) 151 794 6034;

e-mail: annaehrle@googlemail.com

With 6 figures and 1 table

Received December 2016; accepted for publication December 2016

doi: 10.1111/ah.12261

Institution where the work was carried out:
Institute of Veterinary Science University of Liverpool, Philip Leverhulme Equine Hospital, Chester High Road, Neston, CH64 7TE, UK.

Summary

Pain related to the osseous thoracolumbar spine is common in the equine athlete, with minimal information available regarding soft tissue pathology. The aims of this study were to describe the anatomy of the equine SSL and ISL (supraspinous and interspinous ligaments) in detail and to assess the innervation of the ligaments and their myofascial attachments including the thoracolumbar fascia. Ten equine thoracolumbar spines (T15-L1) were dissected to define structure and anatomy of the SSL, ISL and adjacent myofascial attachments. Morphological evaluation included histology, electron microscopy and immunohistochemistry (S100 and Substance P) of the SSL, ISL, adjacent fascial attachments, connective tissue and musculature. The anatomical study demonstrated that the SSL and ISL tissues merge with the adjacent myofascia. The ISL has a crossing fibre arrangement consisting of four ligamentous layers with adipose tissue axially. A high proportion of single nerve fibres were detected in the SSL (mean = 2.08 fibres/mm²) and ISL (mean = 0.75 fibres/mm²), with the larger nerves located between the ligamentous and muscular tissue. The oblique crossing arrangement of the fibres of the ISL likely functions to resist distractive and rotational forces, therefore stabilizing the equine thoracolumbar spine. The dense sensory innervation within the SSL and ISL could explain the severe pain experienced by some horses with impinging dorsal spinous processes. Documentation of the nervous supply of the soft tissues associated with the dorsal spinous processes is a key step towards improving our understanding of equine back pain.

Introduction

Pain related to osseous and soft tissue pathology of the thoracolumbar spine is a common condition in the equine athlete (Denoix and Dyson, 2011). Overriding or impinging DSPs (dorsal spinous processes) and osteoarthritis of the articular process joints are the frequently diagnosed bone-related causes of back pain, usually localized between T15 and L1 (Walmsley et al., 2002; Girodroux et al., 2009; Cousty et al., 2010). Soft tissue lesions are mainly described in the M. longissimus dorsi, M. multifidus and SSL (Jeffcott, 1980; Gillis, 1999; Stubbs et al., 2010).

In man, the TLF (thoracolumbar fascia) is a commonly diagnosed source of non-specific lower back pain (Gibson

et al., 2009; Willard et al., 2012; Schilder et al., 2014). Fascia performs an important role in transmitting mechanical forces between muscles. With acute inflammation, fascia tightens and becomes less flexible (Schleip, 2003). The detailed anatomy and sensory innervation of the TLF, SSL (supraspinous ligament) and ISL (interspinous ligament) have been investigated in man and in other animals; however, there is little information about these tissues in horses (Jiang et al., 1995a; Johnson and Zhang, 2002; Tsao et al., 2010; Tesarz et al., 2011; Hoheisel and Mense, 2015).

The general macroscopic appearances of the equine TLF, SSL and ISL have been described without concurrent description of the microscopic structure (Budras et al.,

2003; Clayton et al., 2005; Liebich and König, 2007). The innervation of the epaxial musculature in horses has been detailed macroscopically to the level of the articular process joints, with little information regarding innervation of the tissues further dorsal (Vandeweerdt et al., 2007). Therefore, the aims of this study were to describe the anatomy of the SSL, ISL and TLF of the equine thoracolumbar spine and to assess the innervation of the ligaments and aponeurotic myofascial layers in microscopic detail. The authors hypothesize that the soft tissues adjacent to the DSPs contain a dense sensory innervation similar to that described in humans.

Materials and Methods

Anatomical study

The thoracolumbar spines of 10 skeletally mature horses (4–18 years) humanely destroyed for reasons unrelated to thoracolumbar pathology were included in the study. Informed owner consent for tissue retention was obtained, and approval for the study was given by the local Committee on Research Ethics. The breeds represented were Thoroughbred (3), Warmbloods (1), Irish Sports Horse (3), Cob (1), Arabian (1) and Lusitano (1). There were six geldings and four mares.

Cadavers were placed in left lateral recumbency and the skin was removed, followed by reflection of the STF

(superficial trunk fascia) and *M. cutaneous trunci*. The fascial attachments of the *M. trapezius*, *M. latissimus dorsi* and *M. longissimus dorsi* were determined before the muscle was separated from the fascia overlying the *M. multifidus*. The fibre arrangement of this fascia was documented before the ventral attachments were transected and the fascia reflected dorsally. The fascicles of the *M. multifidus* were detached from their ventral insertions on the mammillary processes to allow access to the ISLs. Meticulous anatomical dissection was performed to determine the structure and orientation of the ligamentous fibres of the SSL and ISL between T15 and L1. The relationship between different layers of fascia and their origins on the DSPs, the SSL and ISL was documented photographically.

Histological study

One tissue sample of the SSL and interconnecting ISL, including the inserting fascial planes and adjacent musculature, was harvested from each interspinous space between T15 and L1 in each specimen within two hours following euthanasia (Fig. 1). The sections were cut immediately adjacent to the bony margins of the DSPs from the level of the SSL to the most ventral part of the ISL at the intervertebral junction. Samples were fixed in 10% buffered formalin for 48–72 h before being trimmed for paraffin embedding and tissue sectioning. Two slides

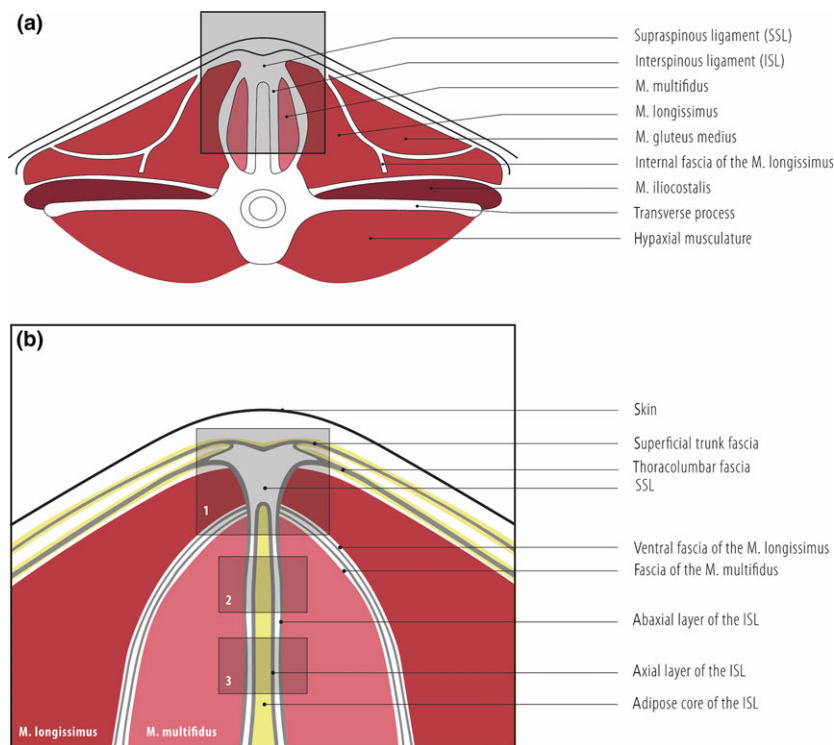


Fig. 1. Schematic illustration of the anatomical connection between the SSL, the ISL and the adjacent myofascial attachments at the level of T18. a. Transverse section of the caudal thoracic spine indicating the area of interest for histomorphological assessment (grey box) b. Detailed illustration of the anatomy and sites for tissue harvesting in the thoracolumbar spinal region. 1 = tissue section harvested from each interspinous spaces T15–L1, containing a transverse section of the SSL including the origin of fascia and muscle layers and the overlying STF. 2 = dorsal transverse section of the ISL. 3 = ventral transverse section of the ISL. Each section includes about 50% ISL and 50% adjacent musculature.

per DSP interface were prepared for histological examination. One slide contained a transverse section of the SSL including the origin of related fascia and muscle layers. The second slide contained a dorsal and a ventral transverse section of the ISL and adjacent musculature (Fig. 1).

Haematoxylin and eosin (H&E) staining was performed for histomorphological evaluation of SSL, ISL, adjacent fascia and muscular tissue. Tissue was categorized as ligamentous, adipose or muscular. Digital photomicrographs were prepared (Nikon Eclipse i80 equipped with Nikon DS 5mc digital camera; 1600 × 1200 pixels) from which the cross-sectional area of the different tissue categories in each slide was determined (Image J, National Institute of Health; Schneider et al., 2012) and the percentage area of each tissue was calculated. Immunohistochemistry was performed following a previously described protocol (Reszel et al., 2015). For the quantitative evaluation of nervous tissue, anti-S100 antibody (rabbit polyclonal anti-S100; Dako; dilution 1:100) was utilized. Nerves were ranked as small (single nerve fibre), medium (bundle of two to five nerve fibres) or large (bundle of ≥ 6 nerve fibres) (Fig. 2c). The number of nerve fibres in collagenous, adipose or muscular tissue was documented, and the neuron density within each tissue type was calculated (nerves/mm²) for each individual tissue section.

With four randomly selected tissue samples of the SSL and ISL, further staining was performed to detect contractile elements using anti-alpha smooth muscle actin [α SMA] (mouse monoclonal clone 1A4; Dako; dilution: 1:300) and anti-desmin (mouse monoclonal clone D33; Dako; dilution: 1:100) antibodies. The presence of non-myelinated sensory nerve endings was investigated with

anti-human/equine Substance P (rabbit polyclonal; Biorbyt; dilution: 1:500). Tissue sections of normal spinal cord including nerve rootlets were used as control for S100 and Substance P, while smooth muscle of intestine served as control for α SMA and desmin.

Four additional sets of ISL and SSL tissue samples were collected from the interspinous spaces between T15 and L1 immediately post-mortem, fixed in glutaraldehyde and processed rapidly for transmission electron microscopy looking for the presence of non-myelinated sensory nerves, as previously described (Finotello et al., 2016).

Statistical analysis

Data were recorded in Excel (Microsoft Inc., Redmond, Washington, USA) and analysed in Minitab 17 Inc. (State College, Pennsylvania, USA) and STATA 14 (StataCorp., College Station, Texas, USA). Descriptive analysis was performed for the nerve distribution in the SSL, ISL and adjacent tissues. Statistically significant differences in nerve fibre density between SSL and ISL sections, recorded tissue types (ligament, fat and muscle), different interspinous spaces (T15-L1) and between specimens were determined using the non-parametric Kruskal–Wallis test followed by the one-sample Wilcoxon signed rank test. *P* values <0.05 were considered significant.

Results

Anatomical study

In the dorsal midline, the superficial trunk fascia (STF) merged with the SSL and the STF of the opposite side

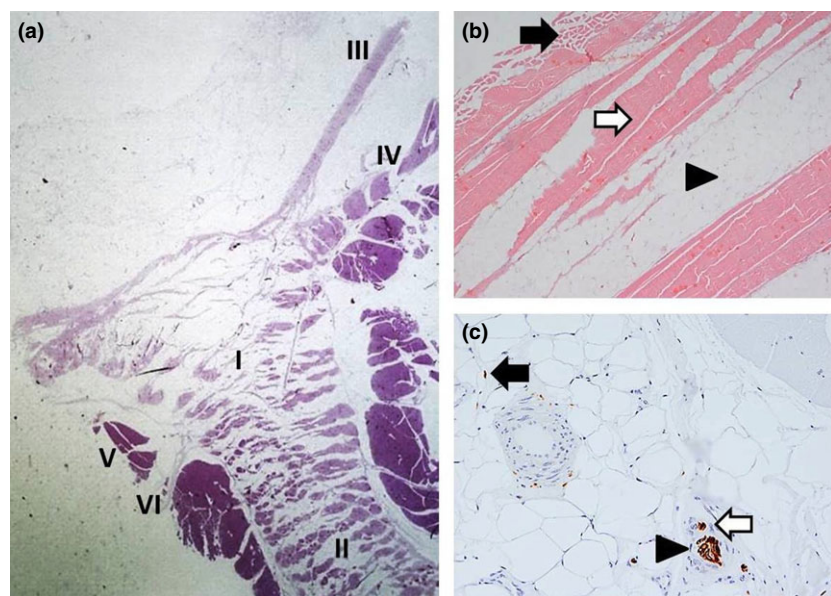


Fig. 2. (a) Haematoxylin and eosin transverse section (20 × magnification) of the SSL with inserting fascial planes (I); ISL (II); STF (III); TLF (IV); M. longissimus dorsi (V); ventral fascia of the M. longissimus (VI). (b) Haematoxylin and eosin (40× magnification) section of the ISL demonstrating the different components: muscle (arrow), ligament (white arrow), adipose tissue (arrowhead) of the ISL. (c) Immunostain S100 (400× magnification) section of the ISL showing loose connective tissue with small (one single nerve fibre; black arrow); medium (bundle of 2–5 nerve fibres; white arrow) and large (bundle of six or more; arrowhead) nerve fibres.

(Figs 1 and 2a). Dorsally, the STF consists of three layers with the superficial and the deep layers composed of areolar tissue with variable amounts of fat deposition (2–10 mm thickness). The middle (main) layer of the STF is largely composed of firm collagenous tissue. Like the STF, the TLF (or deep trunk fascia) consists of three layers, two thin adipose outer layers and one substantial collagenous middle layer. The middle layer is composed of multiple tendinous fascicles, which angle axially to merge into and form a main component of the SSL (Figs 1 and 2a).

The fascia of the *M. latissimus dorsi* merges into the STF in a cranio-abaxial to caudo-axial direction, becoming a major part of the STF. The TLF overlies most of the *M. longissimus dorsi* and may be referred to as the dorsal myofascia of the *M. longissimus dorsi*. In the caudal thoracic and lumbar spine (T17–L5), the *M. longissimus dorsi* is subdivided in a sagittal plane by an internal fascial layer originating from the TLF about 8 to 10 cm abaxial to the dorsal midline (Fig. 1a). The caudal aspect of the *M. longissimus dorsi* between T17 and L5 is covered by the *M. gluteus medius* with the two muscles separated by firm fascia arising from the TLF.

The ventral fascia of the *M. longissimus dorsi* forms fascicles that insert onto the caudal aspect of the articular and mammillary processes of each vertebra in the thoracolumbar spine. The fibre direction of these fascicles is cranioventral to caudodorsal, whereas the multiple fascicles of the *M. multifidus* are oriented from craniodorsal to caudoventral (Fig. 3). The fascicles of the ventral fascia of the *M. longissimus dorsi* span one to two DSPs before they blend into the SSL and the most dorsal aspect of the ISL (Figs 2a and 3). The majority of the segmental fascicles of the *M. multifidus* arise from the caudolateral aspect of the DSPs with some scattered fibres originating

from the abaxial layer of the ISL (Fig. 4). The largest of the segmental muscle bands of the *M. multifidus* cross three to four DSPs before attaching on the cranial aspect of a more caudal mammillary process.

The most dorsal aspect of the SSL consists of the fibres of the STF with the majority of the body of the ligament being composed of a crossing arrangement of the fibres of the merging TLF. The most ventral fibres of the SSL either continue into the ISL or are closely attached to the dorsal DSPs. The structures that merge to form the SSL between T15 and L1 include the STF, TLF, ventral fascia of the *M. longissimus dorsi*, fascicles of the *M. multifidus* and the ISL. The TLF and the ISL fibres make up the majority of the structure of the SSL (Figs 1 and 2a).

The ISL consists of up to four ligamentous sagittal layers that blend into the SSL dorsally. The fibres of the two abaxial ISL layers course between the caudoventral aspect of the rostral DSP and the craniodorsal aspect of the caudal DSP. The fibres of the two axial ISL layers course in the opposite direction, from rostrodorsal to caudoventral (Fig. 4). The abaxial layer is thinner and the fascicles smaller than those of the axial layer. A proportion of the fascicles of the *M. multifidus* and the DSP periosteum merge into the abaxial layers of the ISL. Particularly in the thoracic spine, the abaxial layers of the ISL insert close to the articular process joint capsules. A core of loose adipose tissue lies between the axial ISL ligamentous layers (Fig. 2b).

Histological study

The histological assessment of the SSL and ISL confirmed the previously described close association between the ligaments and adjacent fascial planes (Fig. 2a). A funicular core of the SSL was detected inconsistently in the most cranial section of the ligament (T15–T16) in some

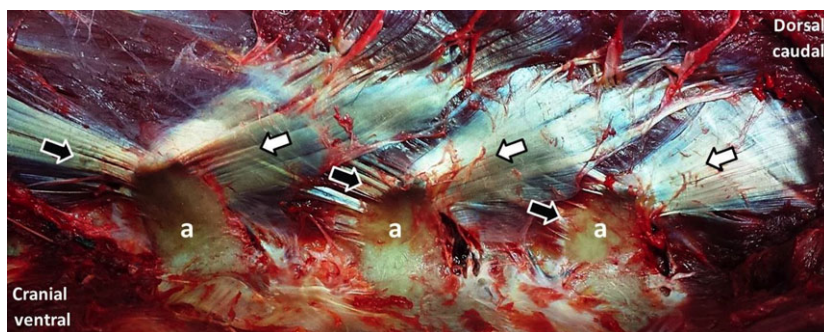


Fig. 3. Photograph of the fascial attachments of the ventral fascia of the *M. longissimus dorsi* (white arrow) and the fascicles of the *M. multifidus* (black arrow) on the vertebral articular processes (a) (T17–L1). The fascicles of the *M. multifidus* arise from the caudal aspect of the DSPs and the abaxial layer of the ISL. The fascicles cross approximately three to four DSPs before they attach on the articular processes in the thoracolumbar spine. The fascicles of the ventral fascia of the *M. longissimus dorsi* have their origin at the caudal aspect of the articular and mammillary processes of each vertebra, overlie the *M. multifidus* fascicles and span one to two DSPs before they blend into the SSL and the most dorsal aspect of the ISL further caudal.

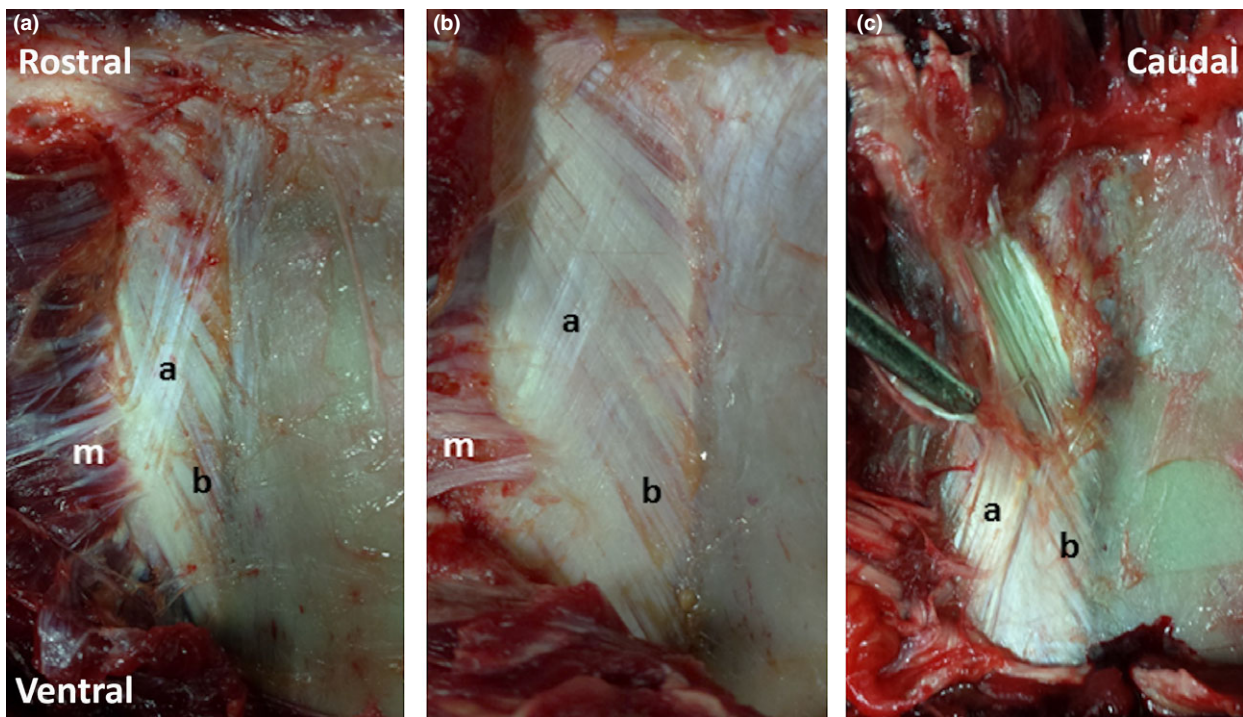


Fig. 4. (a–c) Photographs of the ISL with attachments of the fascicles of the *M. multifidus* (m) to the abaxial layer of the ISL (a), overlying the axial layer of the ISL (b). The fibres of the two abaxial ligamentous layers course between the caudoventral aspect of the rostral DSP and the craniodorsal aspect of the DSP that lies caudal to the ISL. The fibres of the two axial layers course in the opposite direction, from dorsorostral to caudoventral.

horses ($n = 6$) but was not present in the majority of the sections examined ($n = 34$). A clear distinction was not detectable between the fibres of the SSL and ISL in the transition area between the two ligaments. A core of adipose tissue was present in the midline between the axial ISL ligamentous layers (Fig. 2b).

The S100 immunostain revealed distinct single nerve fibres and fascicles in the SSL, ISL, adipose tissue and the musculature (Fig. 2c). The highest density of single nerve fibres was detected in the SSL (2.08 fibres/mm^2) and in the *M. multifidus* (2.35 fibres/mm^2). A high proportion of single nerve fibres was also detected in the ligamentous fibres (0.75 fibres/mm^2) and the adipose core (1.79 fibres/mm^2) of the ISL. Medium and large sized nerves were evident mainly in the loose connective tissue between the SSL, ISL and the *M. longissimus* and *multifidus* (Table 1). Quantitative assessment of nerve fibres did not identify a significant difference in the density of nerve fibres between the tissues sampled from different interspinous spaces ($p = 0.073$). A wide variation of neuron density within the SSL and ISL was found between the different horses ($p = 0.001$). Kappa coefficient indicated good intra- and inter-observer agreement (0.93 and 0.74, respectively) for the quantitative assessment of nerves within the described tissues.

The staining with α SMA and desmin antibodies confirmed that the SSL and ISL were largely free of contractile elements. Very few, scattered small α SMA-positive fibres were detected throughout the sections examined (Fig. 5a). Substance P identified a high number of small nerve endings within the ligamentous tissue of the SSL and ISL, smaller than the single nerve fibres detected with the S100 immunostain (Figs 2c and 5b). Transmission electron microscopy confirmed the presence of cytoplasmic cellular processes consistent with small, sensory nerve endings exhibiting a double membrane and mitochondria within the collagen bundles of the SSL and ISL sections (Fig. 6).

Discussion

The anatomical study demonstrated intimate connection between the SSL, ISL and the myofascia of the equine epaxial musculature. The oblique crossing arrangement of the *M. longissimus dorsi* and *M. multifidus* fibres and the crossed arrangement of the ISL fibres may indicate a shared biomechanical role of these structures, counteracting forces of distraction along the equine thoracolumbar spine. As with human anatomy, a dense sensory innervation was found within the SSL and ISL, with the larger

Table 1. Quantitative assessment of nerve distribution calculated as nerve fibre/mm² within ligament, fat or muscle

Nerves/mm ²	Supraspinous ligament (SSL)			Interspinous ligament (ISL)		
	Ligament	Fat	Muscle	Ligament	Fat	Muscle
<i>Small nerves</i>						
Mean/median	2.08/2.05	1.62/1.39	1.60/1.11	0.75/0.34	1.79/0.85	2.35/2.17
Range	0.05–5.41	0.34–6.49	0.0–7.61	0.0–3.32	0.0–25.52	0.05–6.59
±SD	±1.24	±1.25	±1.81	±0.88	±4.12	±1.8
<i>Medium nerves</i>						
Mean/median	0.19/0.15	0.29/0.25	0.33/0.18	0.10/0.04	0.53/0.21	0.56/0.41
Range	0.0–1.14	0.06–1.25	0.0–2.29	0.0–0.57	0.0–5.0	0.0–2.63
±SD	±0.19	±0.22	±0.44	±0.14	±0.97	±0.6
<i>Large nerves</i>						
Mean/median	0.05/0.04	0.15/0.11	0.10/0.06	0.05/0.01	0.36/0.07	0.22/0.19
Range	0.01–0.15	0.0–0.64	0.0–0.96	0.0–1.04	0.0–4.64	0.0–0.6
±SD	±0.03	±0.13	±0.16	±0.17	±0.82	±0.18

Small = one nerve fibre; medium = 2–5 nerve fibres; large = ≥6 fibres. The muscle adjacent to the SSL represents the M. longissimus dorsi and the muscular tissue adjacent to the ISL consists of the fibres of the M. multifidus.

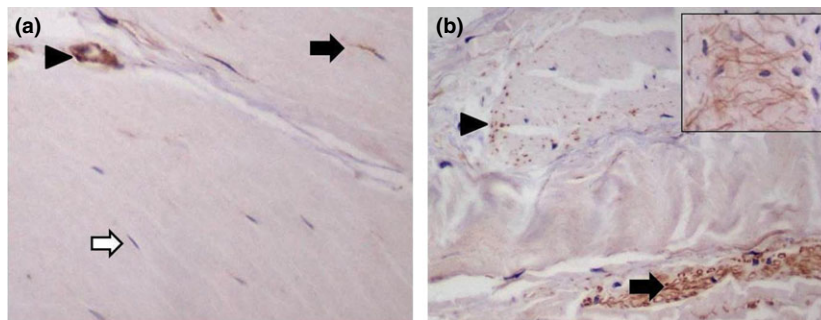


Fig. 5. (a) Alpha smooth muscle actin (α SMA) stain (400 \times magnification) of a section of the SSL between T17 and T18. The density of contractile elements is low within the collagen bundle shown. Black arrow = scattered contractile element. White arrow: negative fibroblast; arrowhead: internal positive control: smooth muscle cells of small blood vessel wall. (b) Section of the ISL between T15 and T16. Using Substance P stain (400 \times magnification), medium sized (arrow) and very small (arrowhead) single fibre nerve endings are present within the ligamentous tissue, smaller than the single nerve fibres that were found using the S100 immunostain. Small Substance P-positive nerve fibres are evident in transversal (arrowhead) or occasionally longitudinal (inset) section.

nerves located in the loose connective and muscular tissue.

The SSL is a well-defined structure with anatomical similarities across a diverse range of species including bipeds, pseudo-bipeds and small quadrupeds (Jiang et al., 1995b). In contrast, the anatomical structure of the ISL varies significantly between species. In the dog and cat, the ISL is poorly developed, except dorsally where a thin double layer of distinct fibres merges with the TLF. A significant difference has been described in the fibre orientation between the ISL in baboons and humans with the well-developed, bilateral elastic fibres of the ISL in the baboon taking a direct craniocaudal course between the DSPs (Heylings, 1980). Like the equine ISL, the human ISL has been shown to be arranged in axial and abaxial layers with a fat filled slit-like midline cavity (Heylings, 1978). As in this study, the majority of the ISL fibres in

humans and pigs are directed from craniodorsal to caudoventral with a thin, superficial layer of fibres directed in caudoventral to craniodorsal direction (Aspden et al., 1987; Scapinelli et al., 2006).

In man, the SSL and ISL maintain spinal stability by providing both mechanical constraint and neuromuscular feedback, while aiding force transmission from the TLF to the vertebrae (Aspden et al., 1987; Yahia et al., 1988). Both ligaments limit mainly the ventral flexion of the thoracolumbar spine in man and may play a similar role in the horse as the caudal thoracic and lumbar spine has been shown to be the least mobile region of the equine back (Prestar, 1982; Townsend et al., 1983; Hindle et al., 1990). In the thoracic spine, lateral bending is always accompanied by axial rotation which is limited by the rib cage (Townsend et al., 1983; Townsend and Leach, 1984; Faber et al., 2001a,b). The oblique crossing arrangement

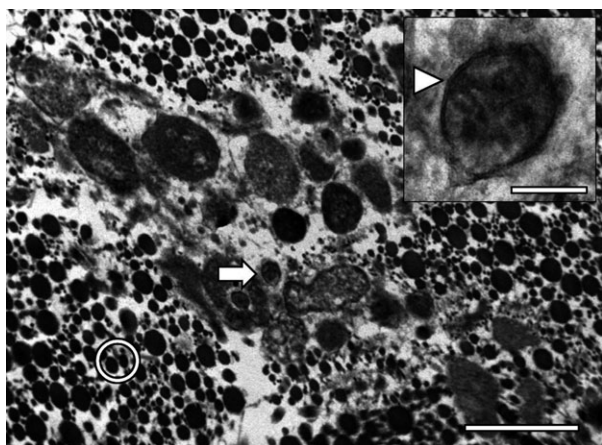


Fig. 6. Transmission electron microscopy image (scale bar = 1 micron) of the ISL at T18-L1. The arrow indicates cytoplasmic processes consistent with terminal unmyelinated fibres, scattered within collagen fibres (white circle). Inset: higher magnification identifies very small cytoplasmic processes characterized by double-layered plasma membrane (arrowhead—scale bar = 150 nm) consistent with small cytoplasmic processes identified by Substance P stain (Fig. 5b).

of fibrous bundles of the equine ISL is likely to counteract tensile and rotational forces of distraction between the DSPs in the caudal thoracic and cranial lumbar spine. Like in humans and other quadrupeds, the *M. multifidus* provides intersegmental stability and stiffness in the equine thoracolumbar spine (Kaigle et al., 1995; Wilke et al., 1995; Stubbs et al., 2010). The close association between the ventral fascia of the *M. longissimus dorsi*, the multifidus fascia and the ISL suggests that all of these structures participate in the core stabilization of the equine thoracolumbar spine.

Similar to the extensive neural network identified in the human SSL, ISL and TLF, the nerve endings identified in the horse likely provide a neurological feedback mechanism for the protection and stabilization of the spine (Jiang et al., 1995a; Scapinelli et al., 2006; Tesarz et al., 2011). In the rat, induced inflammation in the TLF resulted in increased nociceptive input to the lumbar dorsal horn neurons with an increase in nociceptive fibres when compared to controls (Hoheisel and Mense, 2015; Hoheisel et al., 2015). Based on the histological study of the equine SSL, ISL and TLF, the free nerve endings identified adjacent to the collagen fibres are believed to be mainly responsible for the sensory innervation of these tissues. The high number of Substance P-positive free nerve ending when compared to S100-positive nerve bundles indicates a higher prevalence of non-myelinated fibres within the structures examined, which was also confirmed by electron microscopy. In the horse, inflammation in the SSL and ISL associated with muscular pain or as a result of

impingement of the DSPs could potentiate sensory stimulation in this region, explaining the high level of resentment to ridden exercise noted in many of these cases. Clinical studies have suggested that chronically active 'kissing spines' may be associated with desmitis of the ISL or a compartment syndrome in the area of the interspinous space (Coomer et al., 2012). Further work is required to investigate the alteration in sensory innervation in diseased tissue to determine the role of myofascial pain in relation to back pain in horses. In addition, all surgical techniques to treat impinging DSPs in the horse result in trauma to the SSL, ISL and the fascial attachments (Walmsley et al., 2002; Perkins et al., 2005; Coomer et al., 2012). The influence of this disruption on the biomechanics and the nociceptive feedback in the thoracolumbar spinal region has not been explored and could have long-term implications for horses undergoing spinal surgery.

Interestingly, the highest density of small nerve endings was identified in the SSL and *M. multifidus*. The high density of small sensory nerve endings as well as larger, afferent nerves identified in the equine *M. multifidus* is consistent with the neuroanatomical pathway of nociception of the *M. multifidus* described in rats (Taguchi et al., 2007). The significance of the SSL in equine back pathology is controversial, and lesions within the ligament are difficult to diagnose (Henson et al., 2007; Lamas, 2013). Nociceptive fibres within the SSL have been associated with lower back pain in human patients (El-Bohy et al., 1988). Based on the histological study of the equine SSL, pain associated with the SSL may be explained by the ligament's dense sensory innervation.

Conclusion

In summary, the anatomical features described in this study, particularly the oblique crossing fibre arrangement of the ISL layers and the myofascia of the *M. multifidus* and *M. longissimus*, are likely to stabilize the equine thoracolumbar spine and function to resist tensile and rotational forces of distraction along the DSPs. The dense sensory innervation within the SSL and ISL could provide an anatomical basis for the perception of the severe pain experienced by some horses with DSP impingement. The documentation of the anatomical structure and nervous supply of the soft tissues associated with the DSPs is a key step towards improving our understanding of equine back pain.

Acknowledgements

The authors gratefully acknowledge the support of Narelle Stubbs and Gordon Sidlow contributing to the development of the study. We would further like to

thank Peter Cripps for his invaluable role in the statistical analysis of the data and Tony Jopson, Marion Pope and the team of necropsy technicians of the Department for Diagnostic Pathology of the University of Liverpool for their technical assistance. Additionally, we would like to thank Claudia Pintat for her help with the design of the schematic illustration and the Institute of Veterinary Science University of Liverpool for funding this study.

Conflict of Interests

None of the authors has any financial or personal relationships that could inappropriately influence or bias the content of the paper.

Sources of Funding

This research was funded by the Institute of Veterinary Science, University of Liverpool.

Ethical Considerations

Informed owner consent for tissue retention was obtained, and the study was approved by the Veterinary Research Ethics Committee, University of Liverpool.

References

- Aspden, R. M., N. H. Bornstein, and D. W. Hukins, 1987: Collagen organisation in the interspinous ligament and its relationship to tissue function. *J. Anat.* **155**, 141–151.
- Budras, K.-D., W. O. Sack, S. Rock, A. Horwitz, and R. Berg, 2003: Chapter 7: Abdominal wall and Cavity. In: *Abdominal Wall and Cavity Anatomy of the Horse*, 4th edn. Hannover: Schlütersche.
- Clayton, H. M., P. F. Flood, D. S. Rosenstein, and D. Mandeville, 2005: Spinal column. In: *Clinical Anatomy of the Horse*, 1st edn. Philadelphia: Elsevier.
- Coomer, R. P., S. A. McKane, N. Smith, and J. M. Vandeweerd, 2012: A controlled study evaluating a novel surgical treatment for kissing spines in standing sedated horses. *Vet. Surg.* **41**, 890–897.
- Cousty, M., C. Rétureau, C. Tricaud, O. Geffreu, and S. Caure, 2010: Location of radiological lesions of the thoracolumbar column in French trotters with and without signs of back pain. *Vet. Rec.* **166**, 41–45.
- Denoix, J. M., and S. J. Dyson, 2011: Thoracolumbar Spine. In: *Diagnosis and Management of Lameness in the Horse*, 2nd edn. Philadelphia: Elsevier.
- El-Bohy, A., J. M. Cavanaugh, M. L. Getchell, T. Bulas, T. V. Getchell, and A. I. King, 1988: Localization of substance P and neurofilament immunoreactive fibres in the lumbar facet joint capsule and supraspinous ligament of the rabbit. *Brain Res.* **460**, 379–382.
- Faber, M., C. Johnston, H. Schamhardt, R. van Weeren, L. Roepstorff, and A. Barneveld, 2001a: Basic three-dimensional kinematics of the vertebral column of horses trotting on a treadmill. *Am. J. Vet. Res.* **62**, 757–764.
- Faber, M., C. Johnston, H. C. Schamhardt, R. van Weeren, L. Roepstorff, and A. Barneveld, 2001b: Three-dimensional kinematics of the equine spine during canter. *Equine Vet. J. Suppl.* **33**, 145–149.
- Finotello, R., C. Masserdotti, G. Baroni, and L. Ressel, 2016: The role of thyroid transcription factor-1 in the diagnosis of feline lung digit syndrome. *J. Feline Med. Surg.* **2**, 1–7.
- Gibson, W., L. Arendt-Nielsen, T. Taguchi, K. Mizumura, and T. Graven-Nielsen, 2009: Increased pain from muscle fascia following eccentric exercise: animal and human findings. *Exp. Brain Res.* **194**, 299–308.
- Gillis, C., 1999: Spinal ligament pathology. *Vet. Clin. North Am. Equine Pract.* **15**, 97–101.
- Girodroux, M., S. Dyson, and R. Murray, 2009: Osteoarthritis of the thoracolumbar synovial intervertebral articulations: Clinical and radiographic features in 77 horses with poor performance and back pain. *Equine Vet. J.* **41**, 130–138.
- Henson, F. M., L. Lamas, S. Knezevic, and L. B. Jeffcott, 2007: Ultrasonographic evaluation of the supraspinous ligament in a series of ridden and unridden horses and horses with unrelated back pathology. *BMC Vet. Res.* **3**, 3.
- Heylings, D. J. A., 1980: Supraspinous and interspinous ligaments in dog, cat and baboon. *J. Anat.* **130**, 223–228.
- Heylings, D. J. A., 1978: Supraspinous and interspinous ligaments of the human lumbar spine. *J. Anat.* **125**, 127–131.
- Hindle, R. J., M. J. Percy, and A. Cross, 1990: Mechanical function of the human lumbar interspinous and supraspinous ligaments. *J. Biomed. Eng.* **12**, 340–344.
- Hoheisel, U., and S. Mense, 2015: Inflammation of the thoracolumbar fascia excites and sensitizes rat dorsal horn neurons. *Eur. J. Pain.* **19**, 419–429.
- Hoheisel, U., J. Rosner, and S. Mense, 2015: Innervation changes induced by inflammation of the rat thoracolumbar fascia. *Neuroscience.* **6**, 351–359.
- Jeffcott, L. B., 1980: Disorders of the thoracolumbar spine of the horse – a survey of 443 cases. *Equine Vet. J.* **2**, 197–210.
- Jiang, H., G. Russel, V. J. Raso, M. J. Moreau, D. L. Hill, and K. M. Bagnall, 1995a: The nature and distribution of the innervation of human supraspinal and interspinal ligaments. *Spine.* **20**, 869–876.
- Jiang, H., M. Moreau, V. J. Raso, G. Russel, and K. Bagnall, 1995b: A comparison of spinal ligaments – differences between bipeds and quadrupeds. *J. Anat.* **187**, 85–91.
- Johnson, G. M., and M. Zhang, 2002: Regional differences within the human supraspinous and interspinous ligaments: a sheet plastination study. *Eur. Spine J.* **11**, 382–388.
- Kaigle, A. M., N. S. Sten, and T. H. Hansson, 1995: Experimental instability in the lumbar spine. *Spine.* **20**, 420–430.

- Lamas, L., 2013: Chapter 25: Supraspinous ligament and dorsal sacroiliac ligament desmitis. In: *Equine Back Pathology – Diagnosis and Treatment*, 1st edn. Chinchester: Wiley-Blackwell.
- Liebich, H.-G., and H. E. König, 2007: Fascia and muscles of the head, neck and trunk. In: *Fascia Veterinary Anatomy of Domestic Mammals: Textbook and Colour Atlas*, 3rd edn. Stuttgart: Schattauer.
- Perkins, J. D., J. Schumacher, G. Kelly, P. Pollock, and M. Harty, 2005: Subtotal osteotomy of dorsal spinous processes performed in nine standing horses. *Vet. Surg.* **34**, 625–629.
- Prestar, F. J., 1982: Morphology and function of the interspinous ligaments and the supraspinal ligament of the lumbar portion of the spine. *Morphol. Med.* **2**, 53–58.
- Ressel, L., S. Ward, and R. Kipar, 2015: Equine cutaneous mast cell tumours exhibit variable differentiation, proliferation activity and KIT expression. *J. Comp. Pathol.* **153**, 236–243.
- Scapinelli, R., C. Stecco, A. Pozzuoli, A. Porzionato, V. Macchi, and R. De Caro, 2006: The lumbar interspinous ligament in humans: anatomical study and review of the literature. *Cells Tissues Organs.* **183**, 1–11.
- Schilder, A., U. Hoheisel, W. Magerl, and R.-D. Treede, 2014: Sensory findings after stimulation of the thoracolumbar fascia with hypertonic saline suggest its contribution to low back pain. *Pain.* **155**, 222–231.
- Schleip, R., 2003: Fascial plasticity – a new neurobiological explanation: Part 2. *J. Bodyw. Mov. Ther.* **7**, 104–116.
- Schneider, C. A., W. S. Rasband, and K. W. Eliceiri, 2012: NIH Image to ImageJ: 25 years of image analysis. *Nat. Methods.* **9**, 671–675.
- Stubbs, N. C., C. M. Riggs, P. W. Hodges, L. B. Jeffcott, D. R. Hodgson, H. M. Clayton, and C. M. McGowan, 2010: Osseous spinal pathology and epaxial muscle ultrasonography in Thoroughbred racehorses. *Equine Vet. J.* **42**, 654–661.
- Taguchi, T., V. John, U. Hoheisel, and S. Mense, 2007: Neuroanatomical pathway of nociception originating in a low back muscle (multifidus) in the rat. *Neurosci. Lett.* **427**, 22–27.
- Tesarz, J., U. Hoheisel, B. Wiedenhöfer, and S. Mense, 2011: Sensory innervation of the thoracolumbar fascia in rats and humans. *Neuroscience.* **194**, 302–308.
- Townsend, H. G. G., and D. H. Leach, 1984: Relationship between intervertebral joint morphology and mobility in the equine thoracolumbar spine. *Equine Vet. J.* **16**, 461–465.
- Townsend, H. G. G., D. H. Leach, and P. B. Fretz, 1983: Kinematics of the equine thoracolumbar spine. *Equine Vet. J.* **15**, 117–122.
- Tsao, H., K. J. Tucker, M. V. Coppeters, and P. W. Hodges, 2010: Experimentally-induced low back pain from hypertonic saline injections into lumbar interspinous ligament and erector spinae muscle. *Pain.* **150**, 167–172.
- Vandeweerd, J. M., F. Desbrosse, P. Clegg, V. Hougardy, L. Borck, A. Welch, and P. Cripps, 2007: Innervation and nerve injections of the lumbar spine of the horse: a cadaveric study. *Equine Vet. J.* **39**, 59–63.
- Walmsley, J. P., H. Pettersson, F. Winberg, and F. McEvoy, 2002: Impingement of the dorsal spinous processes in two hundred and fifteen horses: case selection, surgical technique and results. *Equine Vet. J.* **34**, 23–28.
- Wilke, H. J., S. Wolf, L. E. Claes, M. Arand, and A. Wiesend, 1995: Stability increase of the lumbar spine with different muscle groups. A biomechanical in vitro study. *Spine.* **20**, 192–198.
- Willard, F. H., A. Vleeming, M. D. Schuenke, L. Danneels, and R. Schleip, 2012: The thoracolumbar fascia: anatomy, function and clinical considerations. *J. Anat.* **221**, 507–536.
- Yahia, L. H., N. Newman, and C. H. Rivard, 1988: Neurohistology of lumbar spine ligaments. *Acta Orthop. Scand.* **59**, 508–512.